INFN - Laboratori Nazionali di Frascati, May 1995
From: **The Second DaΦne Physics Handbook**[1]
Chapter 10: Two Photon Processes
Eds. L. Maiani, G. Pancheri, N. Paver

QED Radiative Corrections and Radiative Bhabha Scattering at DAΦNE

M. Greco [a], **G. Montagna** [b], **O. Nicrosini**[c] [2], **F. Piccinini** [d]

a Dipartimento di Fisica, Università de L'Aquila and INFN, Laboratori Nazionali di Frascati, Italy

b INFN, Sezione di Pavia, Italy

c CERN, TH Division, Geneva, Switzerland

d Dipartimento di Fisica Nucleare e Teorica, Università di Pavia and INFN, Sezione di Pavia, Italy

Abstract

Some basics issues of the electromagnetic radiative corrections to e^+e^- collisions at DAΦNE energies are reviewed in the framework of the QED structure function approach. Illustrative numerical results for the Φ line–shape and leptonic pair production over a realistic experimental set–up are given. A phenomenological analysis of radiative Bhabha scattering, with particular emphasis on the very forward region, is also addressed. Predictions for the tagging configurations of interest for the two–photon physics at DAΦNE are given and compared with previous and very recent calculations.

[1]Supported by the INFN, by the EC under the HCM contract number CHRX-CT920026 and by the authors home institutions

[2]On leave from INFN, Sezione di Pavia, Italy.

1 Introduction

It is well known that the proper treatment of QED radiative corrections at e^+e^- colliders constitutes the essential tool to proceed from data taking to the physics analysis because of their large effects on the measured observables. Generally, they depend upon the details of the experiments via the cuts applied to the final state particles and therefore they need much attention for precision measurements. Furthermore, the crucial role played by radiative effects in the production of narrow states has been emphasized since long time [1]. For these reasons, our aim here is to provide a simple and general recipe which can be used for the evaluation of QED corrections to the cross sections of leptonic and hadronic pair production in e^+e^- annihilations over a realistic experimental set–up for DAΦNE physics.

In particular this paper is devoted to discuss the basic issues of two distinct subjects of interest for the experiments planned at the Φ–factory DAΦNE: the electromagnetic radiative corrections to e^+e^- collisions around the Φ peak and the process of (single) radiative Bhabha scattering $e^+e^- \to e^+e^-\gamma$.

The formulation of $e^+e^- \to f\bar{f}(n\gamma)$ processes at $\sqrt{s} \simeq M_\Phi$ is based on recent analyses [2, 3] where a semi–analytical and "realistic" (i.e. including the effects of energy or invariant mass cuts, scattering angle and acollinearity cuts) approach is described in detail and successfully applied to fit electroweak precision data for cross sections and asymmetries around the Z^0 peak. In this sense, we will update and generalize to more realistic set–up the treatment of radiative corrections summarized in the contribution [4] to the first edition of the DAΦNE Physics Handbook, providing also numerical results together with an estimate of the associated theoretical uncertainty.

Radiative Bhabha scattering, which we will discuss next, is relevant at DAΦNE because this process constitutes a very serious background for $\gamma\gamma$ physics experiments with tagging facilities. Precise predictions are therefore mandatory and they require particular care for the presence of extreme (i.e. very forward) angular configurations in the planned tagging devices. Previous analyses, and in particular very recent analytical results, will be reviewed and compared with respect to their physics input as well as their numerical results.

2 Born cross sections for $e^+e^- \to (\gamma, \Phi) \to f\bar{f}$

In this section we report, for the sake of completeness, the lowest order differential cross sections for the processes of fermionic pair production $e^+e^- \to (\gamma, \Phi) \to f\bar{f}$ $(f = e, \mu, q)$ considered in the first two sections of the article. The pure photon, interference and resonant contributions in the s–channel annihilation are given by the well–known formulae:

$$\frac{d\sigma_0}{d\Omega}\Big[\gamma(s),\, \gamma(s)\Big] = \frac{\alpha^2}{4s} Q_f^2 (1 + c^2) \tag{1}$$

$$\frac{d\sigma_0}{d\Omega}\Big[\gamma(s),\, \Phi(s)\Big] = \frac{\alpha^2}{2s} Q_f (1 + c^2) r_v \mathrm{Re}\, \chi(s) \tag{2}$$

$$\frac{d\sigma_0}{d\Omega}\Big[\Phi(s),\, \Phi(s)\Big] = \frac{\alpha^2}{4s} r_v^2 (1 + c^2) |\, \chi(s)\, |^2, \tag{3}$$

where $c = \cos\vartheta$ is the fermion scattering angle and $\chi(s)$ the Φ resonant propagator:

$$\chi(s) = v_e^2 \frac{s}{s - M_\Phi^2 + iM_\Phi\Gamma_\Phi}. \tag{4}$$

Q_f is the fermion electric charge (in electron units), r_v is the ratio of the fermion and electron coupling v_f and v_e to the Φ, i.e. $r_v = v_f/v_e$. The effective couplings v_e, v_f can be simply derived from the measured widths through the tree level relation:

$$\Gamma(\Phi \to f\bar{f}) = \frac{\alpha}{3} v_f^2 M_\Phi. \tag{5}$$

For the process of Bhabha scattering the lowest order contributions due to t–channel γ exchange can be taken into account by adding to the previous formulae (1)–(3) the following ones:

$$\frac{d\sigma_0}{d\Omega}\Big[\gamma(s),\,\gamma(t)\Big] = -\frac{\alpha^2}{2s}\frac{(1+c)^2}{1-c} \tag{6}$$

$$\frac{d\sigma_0}{d\Omega}\Big[\gamma(t),\,\gamma(t)\Big] = \frac{\alpha^2}{4s}\frac{2}{1-c^2}\Big[(1+c)^2+4\Big] \tag{7}$$

$$\frac{d\sigma_0}{d\Omega}\Big[\Phi(s),\,\gamma(t)\Big] = -\frac{\alpha^2}{2s}\frac{(1+c)^2}{1-c}\mathrm{Re}\,\chi(s). \tag{8}$$

The above equations allow to compute the Born cross sections for leptonic pair production and include the inclusive production (Φ line–shape) as a particular case. Furthermore, they can also be used for hadronic $\pi^+\pi^-, K^+K^-, K^0\overline{K}^0$ final states provided that appropriate π and K form factors are supplied as in [4].

3 QED corrections to e^+e^- collisions

Within the QED structure function approach [5, 6], successfully applied nowadays to the evaluation of the electromagnetic corrections to various high–energy reactions of experimental interest, the cross section of a $e^+e^- \to X$ annihilation including initial state radiation is written, according to a QCD analogy to the Drell–Yan process, as convolution of the following form:

$$\sigma_c(s) = \int dx_1 dx_2 D(x_1,s) D(x_2,s) \sigma_0\Big(x_1x_2s\Big). \tag{9}$$

Eq. (9) is based on the factorization theorems [7] of the infrared and collinear singularities: actually, $\sigma_0(x_1x_2s)$ is the hard–scattering cross section (at the reduced energy scale $x_1x_2s = s'$) containing the details of the short–range interaction and $D(x,s)$ represents the probability of finding inside a parent electron (positron) an electron (positron) with a momentum fraction x and virtualness s. Therefore, the structure functions $D(x,s)$ contain the long–distance (universal) logarithmic contributions, due to the soft and/or collinear photon

radiation, which are naturally resummed to all orders when solving the Renormalization Group equation satisfied by the structure function in the non singlet approximation.

In the following, we describe the theoretical ingredients needed to treat, in the framework of QED structure function method, two experimental configurations of typical experimental interest:

- Extrapolated set–up, i.e. when only an invariant mass cut is applied;
- Realistic set–up, i.e. in the presence of energy or invariant mass thresholds, angular acceptance and acollinearity cuts.

3.1 Extrapolated set–up

The treatment of photonic corrections is particularly simple when no realistic cut is imposed in data taking – but an invariant mass one – and therefore the experimental analysis is limited to the so–called extrapolated observables. Actually, for such a configuration, one of the two integrations over the radiative variables x_1 and x_2 in eq. (9) can be analytically performed and the initial state corrected cross section is given by the following one–dimensional convolution formula [5, 6]:

$$\sigma_c(s) = \int_0^{1-\varepsilon} dx H(x,s) \sigma_0\Big((1-x)s\Big), \tag{10}$$

where $\sigma_0(s)$ is the total Born cross section of the specific hard scattering process under consideration. The parameter ε is defined by:

$$\varepsilon = 4\,\frac{m_f^2}{s}, \tag{11}$$

when including the whole photon phase space and can be used to account for a cut on the invariant mass after initial state radiation $\hat{s}$ by replacing $4m_f^2$ with the cut s_0. $H(x,s)$ is known as the *radiator* and it gives the probability that a fraction x of the center of mass energy s is carried away by initial state radiation (up to some photon energy resolution $\frac{\Delta E}{E} = 1-\varepsilon$). The radiator is a universal (process independent) quantity linked to the structure functions by the relation:

$$H(x,s) = \int_{1-x}^1 \frac{dz}{z} D(z,s) D\Big(\frac{1-x}{z}, s\Big). \tag{12}$$

Its explicit expression reads as follows [6]:

$$\begin{aligned} H(x,s) &= (1+\delta)\,\beta\, x^{\beta-1} - \tfrac{1}{2}\,\beta\,(2-x) + \tfrac{1}{8}\,\beta^2 \\ &\times \Big\{(2-x)\,[3\,\ln(1-x) - 4\,\ln x] - \frac{4}{x}\,\ln(1-x) - 6 + x\Big\}, \end{aligned} \tag{13}$$

with

$$\beta = 2\,\frac{\alpha}{\pi}\,(L-1), \qquad L = \ln\frac{s}{m_e^2}. \tag{14}$$

The first exponentiated term takes into account soft multiphoton emission and the second and third terms describe hard bremsstrahlung up to $\mathcal{O}(\alpha^2)$. The factor δ reabsorbs next–to–leading (process dependent) corrections not kept under control by the approach which can be however included by relying upon explicit perturbative calculations. For instance, for a pure $s-$channel resonant cross section, δ is given by the following $\mathcal{O}(\alpha^2)$ factor:

$$\begin{aligned}\delta &= \frac{\alpha}{\pi}\left(\tfrac{3}{2}\,L + \tfrac{\pi^2}{3} - 2\right) + \left(\frac{\alpha}{\pi}\right)^2 \left\{\left(\tfrac{9}{8} - \tfrac{\pi^2}{3}\right) L^2 \right. \\ &+ \left. \left[\left(-\tfrac{45}{16} + \tfrac{11}{12}\,\pi^2 + 3\,\zeta(3)\right] L - \tfrac{9}{2}\,\zeta(3) - \pi^2\,\ln 2 + \tfrac{19}{144}\,\pi^2 + \tfrac{57}{12}\right\}, \qquad (15)\end{aligned}$$

where ζ is the Riemann function. The $K-$ factor (15) comes from the infrared cancellation between the two–loop electron form factor and soft double bremsstrahlung. In the limit of small photon energy resolution, eq. (10), which is currently used by the LEP collaborations to analyze the so–called *perfect data* of LEP 1 processes, reduces to the results of the coherent state approach [8] in terms of infrared factors to all orders and finite order next–to–leading corrections.

For the extrapolated set–up, final state radiation can be easily included by multiplying the kernel cross section by a factor $1 + \delta_{fs}$ obtained by computing the exact $\mathcal{O}(\alpha)$ matrix element for s–channel $e^+e^- \to f\bar{f}\gamma$ (where the photon is emitted by the final state only) and integrating it over the phase space allowed by cuts [9]. If we assume that only an invariant mass cut such as $M^2(f\bar{f}) > \mu_f^2$ is present, the following correction factor has to be included:

$$\begin{aligned}\delta_{fs} &= \frac{\alpha}{\pi}\,Q_f^2 \left\{ - \left[x + \tfrac{1}{2}\,x^2 + 2\,\ln(1-x)\right] \ln\frac{m_f^2}{s} \right. \\ &+ \left. x\,\left(1 + \tfrac{1}{2}\,x\right) \ln\,x + 2\,\ln(1-x)\,(\ln\,x - 1) + 2\,\mathrm{Li}_2(x)\right\}, \qquad (16)\end{aligned}$$

where $x = \mu_f^2/s$. When no cuts at all are applied, δ_{fs} reduces to the well–known and very small $\mathcal{O}(\alpha)$ factor $3/4\,\alpha/\pi\,Q_f^2$.

3.2 Realistic set–up

Computing QED corrections over a realistic set–up is a much more involved problem, since the corrections, besides being large, critically depend on the experimental cuts such as energy or invariant mass thresholds, angular acceptance, acollinearity cut and so on. In this case, the structure function approach allows to write the corrected cross section in the laboratory frame in the following form [2, 3]:

$$\begin{aligned}\sigma_c(s) &= \int_R d\Omega \int_{\Gamma(\Omega)} dx_1 dx_2 D(x_1,s) D(x_2,s) J(x_1,x_2,\vartheta) \\ &\times \frac{d\sigma_0}{d\Omega}(\hat{s}(x_1,x_2), \hat{t}(x_1,x_2,\vartheta)) F_{cut}(\hat{s}(x_1,x_2)), \qquad (17)\end{aligned}$$

where the angular integration has to be understood as follows:

$$\int_R d\Omega = \int_0^{2\pi} d\varphi \int_{\cos(\pi-\vartheta_{min})}^{\cos\vartheta_{min}} d\cos\vartheta, \qquad (18)$$

with φ and ϑ the azimuthal and polar angle of the scattered fermion. Here we limit ourselves to give a general description of eq. (17). For more details and explicit formulae the reader is referred to [2, 3]. $\Gamma(\Omega)$ stands for the portion of the $x_1 - x_2$ initial state radiation phase space allowed by realistic cuts; it can be analytically delimited by solving the kinematics of the hard scattering process in the presence of initial state radiation if one assumes soft and/or collinear approximation and hence derives the limits on the x_1, x_2 variables imposed by realistic cuts. $J(x_1, x_2, \vartheta)$ is the Jacobian of the transformation from the centre of mass to the laboratory frame and accounts for the boost caused by the emission of unbalanced radiation by the initial state radiation. In the ultrarelativistic approximation its expression reads:

$$J(x_1, x_2, \vartheta) \; = \; \frac{x_1 x_2}{\left(x_1 \sin^2 \frac{\vartheta}{2} + x_2 \cos^2 \frac{\vartheta}{2} \right)^2}. \tag{19}$$

The photonic content of the structure function $D(x, s)$ can be directly read by its explicit expression [6]:

$$\begin{aligned} D(x,s) \;\; &= \;\; \delta' \frac{1}{2} \beta (1-x)^{\frac{1}{2}\beta - 1} - \frac{1}{4}\beta(1+x) + \frac{1}{32}\beta^2 \Big[-4(1+x)\ln(1-x) \\ &+ \;\; 3(1+x)\ln x - 4\frac{\ln x}{1-x} - 5 - x \Big], \end{aligned} \tag{20}$$

which one obtains by solving, according to well–established techniques [6], the Lipatov – Altarelli – Parisi evolution equation satisfied by $D(x, s)$ in terms of the one–loop expression for the splitting function *electron* $\rightarrow$ *electron* + *photon*. This allows to resum large mass logarithms from soft multiphoton emission and to include hard photon effects up to $\mathcal{O}(\alpha^2)$. In the K–factor δ' one reabsorbs next–to–leading contributions matching the perturbative results for the specific process under consideration.
$F_{cut}(s)$ provides the final state QED correction to the cross section in the presence of realistic experimental cuts. Its $\mathcal{O}(\alpha)$ analytic expression is known but it is too lengthy to be displayed here and can be found in [9]. It should be emphasized that in a realistic set–up higher order final state corrections could become relevant pointing out the need of introducing a resummation procedure of large logarithms. A detailed discussion about different prescriptions for treating higher order final state effects is given in [2, 3]. Moreover, when considering final state corrections to Bhabha scattering, one is also faced with the problem of the calorimetric measurement for electrons since what is detected is an *electromagnetic jet* of semi–aperture δ_c, where δ_c is an experimental parameter describing the resolution power of the calorimeter. In our approach this effect is accounted for by adding to the $\mathcal{O}(\alpha)$ part of the final state QED correction the contribution due to the emission of an hard photon with an energy fraction greater than $1 - x$, where x is s_0/s for an invariant mass cut and $2E_0/\sqrt{s}$ for an energy threshold cut, and collinear with the final fermion within an angle $0 \leq \vartheta_\gamma \leq \delta_c$. For high–energy electrons the contribution reads [10]

$$F_{coll} \;\; = \;\; 2\,\frac{\alpha}{\pi}\,C,$$

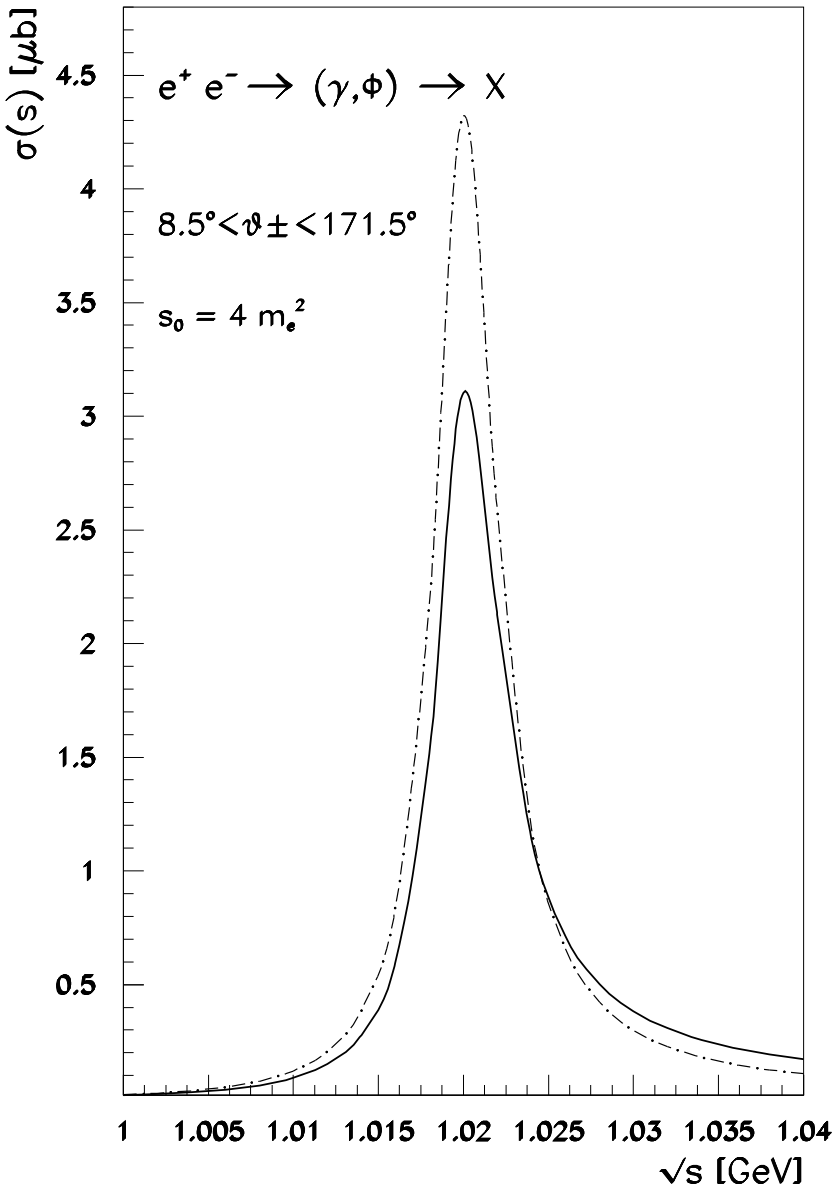

Figure 1: The Φ line–shape over the KLOE angular acceptance and for an invariant mass cut $s_0 = 4m_e^2$. The solid line is the lowest order cross section, the dot–dashed line is the QED corrected cross section.

$$
\begin{aligned}
C &= -\ln(1-x)\Big[\ln\left(1+r^2x^2\right)-1\Big] \\
&+ \Big[\frac{1}{4}-\Big(1-\frac{1}{2}(1-x)\Big)^2\Big]\ln\left(1+r^2x^2\right) \\
&+ \frac{\pi^2}{3}+\frac{9}{4}-\frac{5}{2}(1-x)+\frac{1}{4}(1-x)^2 \\
&+ 2\ln x\ln(1-x)+2\mathrm{Li}_2(1-x), \qquad (21)
\end{aligned}
$$

where

$$
r=\frac{\delta_c\sqrt{s}}{2m_e}. \qquad (22)
$$

Eq. (21) is valid in the approximation $\delta_c \ll 1$ rad and $r \gg 1$ which is safely satisfied at DAΦNE energies.

The master formula (17) needs further manipulations in order to extract numerically stable and fast predictions. Indeed this expression as it stands exhibits several computational problems which can be solved by an appropriate regularization procedure, described in detail in [3], namely the variance–reducing technique known as "control variates". Then the corrected cross section can be written as the the sum of an analytical term, of a one–dimensional integral in the radiator form (containing the bulk of the whole contribution) and terms with one–, two– and three–dimensional integrals controlling the angular and acollinearity effects which, albeit important, are generally a small contribution as compared with the effect due to an invariant mass cut alone. The above regularization procedure is implemented in the FORTRAN program for electroweak physics at LEP/SLC energies `TOPAZ0` [11].

A few comments are in order here about the accuracy of the theoretical predictions derivable from eq. (17) for resonant and non resonant hard scattering processes measured over a realistic set–up. Actually, it should be noted that, whereas any e^+e^- large angle process (including Bhabha scattering) at LEP/SLC energies is a resonant process with small non–resonant contributions, this is not the case of leptonic production at DAΦNE. As a consequence, non leading contributions not included in our approach (initial state hard photon constant terms and initial–final state interference) are almost negligible (of order, say, few 0.1%) only for the case of the Φ line–shape where the above effects are strongly suppressed by the very narrow width of the Φ resonance. This argument obviously does not apply to non–resonant processes $e^+e^- \to \mu^+\mu^-, e^+e^-$ at DAΦNE and therefore the theoretical error, depending on the cuts, becomes larger (presumably of order of a few per cent) and the predictions have to be understood (especially for Bhabha scattering) as leading log ones.

Illustrative numerical results are given in Fig. 1 (Φ line–shape) and Fig. 2 (muon pair cross section) obtained by fitting the program `TOPAZ0` to DAΦNE processes. Fig. 1 shows the lowering of the peak cross section (of order 30%) essentially due soft multiphoton emission and the radiative tail above the peak as a typical convolution hard photon effect. Fig. 2 shows the effects of the QED radiative corrections on the cross section for muon pair production when a realistic experimental set–up is considered.

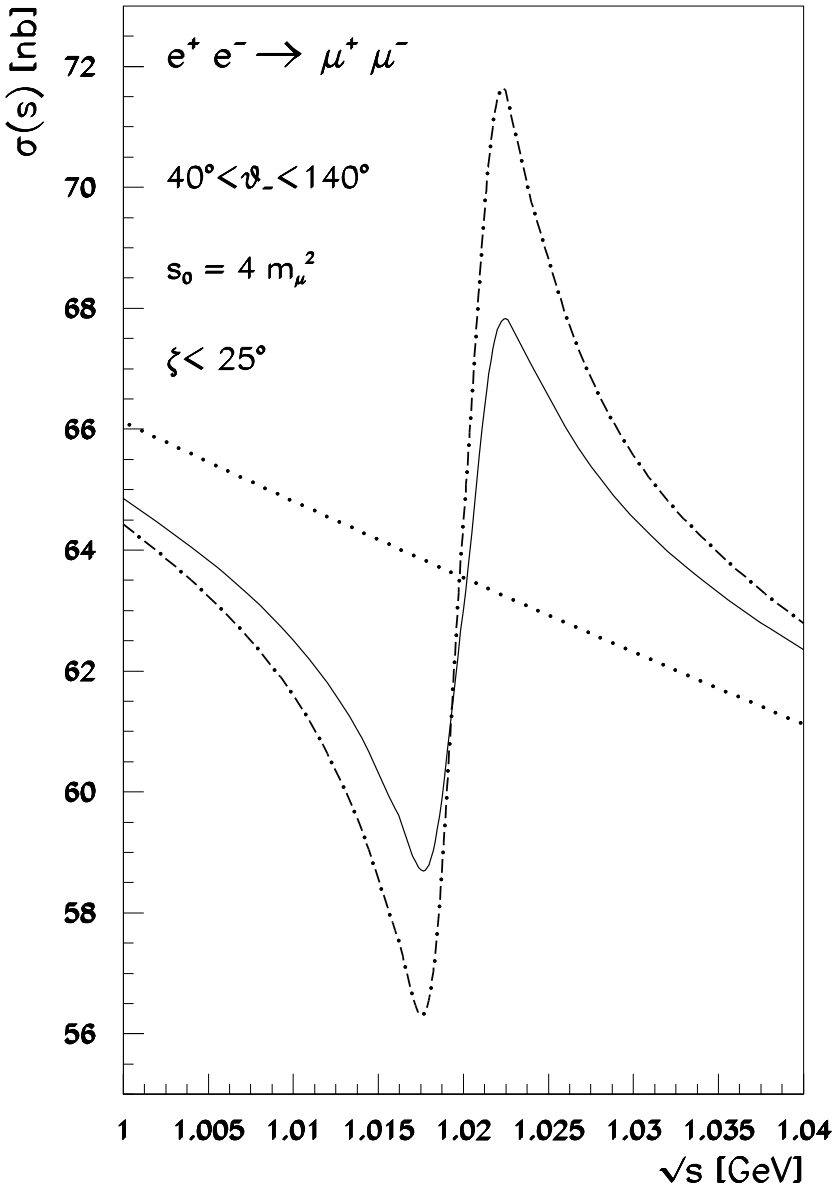

Figure 2: Total cross section of μ–pair production over a realistic experimental set–up ($40^o \leq \vartheta_- \leq 140^o, 0^o \leq \vartheta_+ \leq 180^o, s_0 = 4m_\mu^2$, acollinearity cut $\zeta \leq 25^o$). The dotted line is the QED corrected photon exchange contribution to the muon pair cross section; the dot–dashed line is the sum of the dotted line result with Φ and $\gamma - \Phi$ contributions at Born level; the solid line is the QED corrected total cross section.

4 Radiative Bhabha scattering

In the context of the experiments at the Φ–factory an accurate knowledge of the radiative Bhabha scattering cross section is mandatory because the process constitutes the main background for $\gamma\gamma$ physics experiments with tagging facilities [12, 13]. Theoretical predictions are required for various experimental configurations which include an extremely very forward angular set–up, as can be seen from the following list:

- the cross section in the region $0 \leq \vartheta_- \leq \vartheta_-^{max}$, $E_-^{min} \leq E_- \leq E_-^{max}$, with $\vartheta_-^{max} \geq$ few mrad, $E_-^{min} \simeq 200$ MeV and $E_-^{max} \simeq 450$ MeV, both totally inclusive on the positron and the photon and with acceptance cuts on them (this includes: single tagging rates for small angle scattered electron (SAST), double tagging rates for both electron and positron at small angle (SADT), coincidence rate of electron and photon in the forward direction (SAEPC));

- the cross section for the light spot (LS), i.e. photons detected in the forward direction with energy $E_\gamma \geq k_0$, with k_0 of order few MeV;

- the cross section for the electron in the small angle region defined above and the positron at large angle (SLDT), in particular in the region covered by the detector KLOE [14] ($8.5^\circ \leq \vartheta_+ \leq 171.5^\circ$);

- the cross section for both electron and positron at large angle ($8.5^\circ \leq \vartheta_\pm \leq 171.5^\circ$), but accompanied by a photon of energy $E_\gamma \geq E_\gamma^{min}$ at a minimum angle δ from any of the final state fermions (LLDT).

Although analytic results for differential and total cross sections of $e^+e^- \to e^+e^-\gamma$ are available in the literature (refs. [15]–[17] is an indicative list of such calculations), a detailed analysis of all single and double tagging configurations demands an exact evaluation of the matrix element in the very forward direction, where the momentum transfer is of order m^6/E^4 and the e, γ scattering angles $\vartheta(e,\gamma) \leq 1/\gamma$, with $\gamma = E/m \simeq 10^3$ at DAΦNE.

Unfortunately, in these extreme kinematical conditions the squared matrix element of ref. [18], with the finite mass corrections obviously included, is inapplicable, namely it leads to an unphysical negative result for hard photon emission collinear to the very forward electron direction. Indeed, as discussed in [19], the CALKUL collaboration's result [18] is valid only in the limit $|t| \gg m^2$ whereas in the very forward direction the minimum four–momentum exchange t_{min} is given by:

$$|t_{min}| = \frac{m^6 x^2}{s^2(1-x)^2}, \qquad x = E_\gamma/E, \tag{23}$$

up to $O(m^6)$. Moreover, as a consequence of the approximation used in ref. [18], "off–diagonal" terms of the form $m^2/(p_-\cdot k)/(q_-\cdot k)$, associated to initial–final state interference, are missing. However, for very small electron scattering angles they become of the same order of "diagonal" terms $m^2/(p_- \cdot k)^2$ or $m^2/(q_- \cdot k)^2$ describing initial and final state

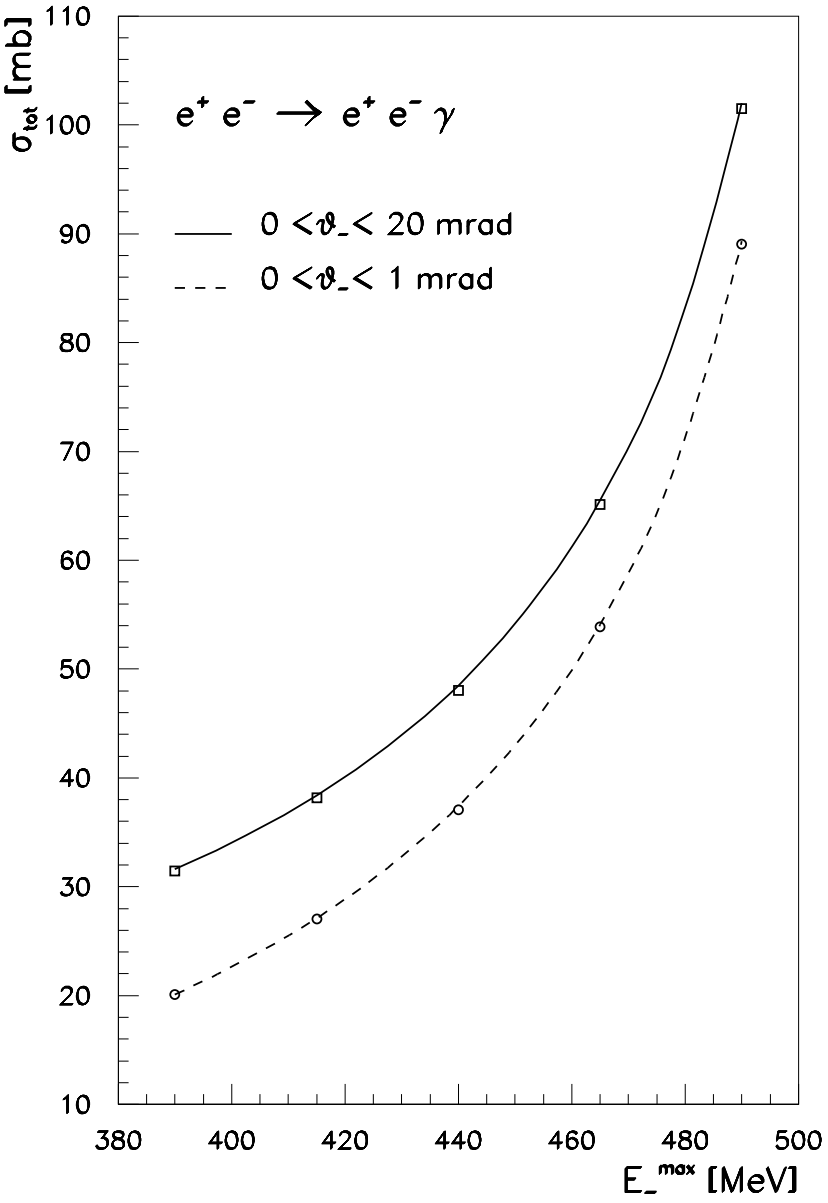

Figure 3: Total cross section of small angle single tagging at DAΦNE, obtained by integrating the electron scattering angle in the range $0 \leq \vartheta_- \leq 1$ mrad (dashed line) and $0 \leq \vartheta_- \leq 20$ mrad (solid line), and the electron energy within $\Delta E_- = E_-^{max} - E_-^{min} = 190$ MeV as a function of the maximum electron energy E_-^{max}. The open circles and squares are the results of the present analysis; the solid and dashed lines correspond to the integration of the spectrum of ref. [16].

radiation respectively. This is due to the fact that in the very forward region initial and final radiation cones overlap and interfere and therefore the contribution of "off–diagonal" mass terms become more and more important when the electron scattering angle goes to zero.

For the above reasons, we computed by using SCHOONSCHIP [20] the complete squared matrix element of the (gauge invariant) t–channel diagrams associated with electron radiation. Positron radiation and electron and positron interference can be safely neglected being suppressed by the stringent constraints on the electron energy. Then the full expression for the squared matrix element, including all $\mathcal{O}(m^2)$, $\mathcal{O}(m^4)$ and $\mathcal{O}(m^6)$ terms, reads as follows [19]:

$$|M|^2 = \frac{2(4\pi\alpha)^3}{t^2}\Big\{ M_0 + m^2 M_2 + m^4 M_4 + m^6 M_6 \Big\}, \tag{24}$$

where

$$\begin{aligned}
M_0 &= -\frac{t}{h_i h_f}[s^2+u^2+t(s+u)+t^2] \\
&- \frac{2t}{h_i}(s+h_f+t) - \frac{2t}{h_f}(-u+h_i-t), \qquad (25)\\
M_2 &= -\frac{1}{h_i^2}[2tu+4h_ih_f+t(4h_i+t)] \\
&- \frac{1}{h_f^2}[2st+4h_ih_f+t(-4h_f+t)] \\
&+ \frac{2t(s+u)}{h_ih_f} - 2\left(\frac{u}{h_i}+\frac{s}{h_f}\right)^2, \qquad (26)\\
M_4 &= 8\left[\frac{s}{h_f^2}+\frac{u}{h_i^2}+\frac{s+t+u}{h_ih_f}\right], \qquad (27)\\
M_6 &= -8\left(\frac{1}{h_i}+\frac{1}{h_f}\right)^2, \qquad (28)
\end{aligned}$$

with $h_i = -p_- \cdot k$, $h_f = -q_- \cdot k$. The other invariants are defined as follows:

$$\begin{aligned}
s &= (p_+ + p_-)^2, \quad t = (p_+ - q_+)^2, \quad u = (p_+ - q_-)^2, \\
s' &= (q_+ + q_-)^2, \quad t' = (p_- - q_-)^2, \quad u' = (p_- - q_+)^2,
\end{aligned}$$

where $p_{-(+)}$ and $q_{-(+)}$ are the four–momenta of the incoming and outgoing electron (positron). The squared matrix element (24) coincides with the result obtained independently in [21].

Based on the analytic result (24), the semi–analytical program PHIPHI [22] has been developed in order to obtain phenomenological predictions of interest at DAΦNE. Some results are shown in Fig. 3 – 5 together with comparisons with those existing in the literature.

In Fig. 3 the total cross section of small angle single tagging at DAΦNE obtained by integrating the electron energy over the range $\Delta E_- = E_-^{max} - E_-^{min} = 190$ MeV is shown as a function of the maximum electron energy E_-^{max}. The solid and dashed lines correspond to the integration of the spectrum $d^2\sigma/dE_-d\vartheta_-$ of ref. [16] in two different domains of the electron scattering angle, namely $0 \leq \vartheta_- \leq 1$ mrad (dashed line) and $0 \leq \vartheta_- \leq 20$ mrad (solid line). Our results are represented by the open circles and squares showing a fully satisfactory agreement with the integration of the analytical result of [16]. For the energy and angle intervals of interest at DAΦNE, i.e. $210 \leq E_- \leq 400$ MeV and $250 \leq E_- \leq 440$ MeV with $\vartheta_-^{max} = 20$ mrad the total cross section is about 35, 50 mb respectively.

Fig. 4 shows a comparison for the total cross section of SAST between the recent results of ref. [23] and ours obtained with $0 \leq \vartheta_- \leq 1$ mrad , $0 \leq \vartheta_- \leq 2$ mrad and $0 \leq \vartheta_- \leq 20$ mrad and the electron energy within $\Delta E_- = E_-^{max} - E_-^{min} = 190$ MeV, as a function of the maximum electron energy E_-^{max}. More in detail, in ref. [23] an approximate formula for the total cross section of SAST in the forward region, with a radiative energy loss of at least ΔE and momentum transfer in the range t_0 and t_1, is given as:

$$\sigma_{tot} = \int_{\Delta E}^{E} dk \int_{t_0}^{t_1} dt \frac{d\sigma}{dkdt} \tag{29}$$

with

$$\frac{d\sigma}{dkdt} \simeq 4\pi\alpha^2 \frac{dt}{t^2}\beta(t)\frac{dk}{k}\frac{E^2+(E-k)^2}{2E^2}, \tag{30}$$

and the function $\beta(t)$ takes the form:

$$\beta(t) = \frac{4\alpha}{\pi}\Big(\frac{2m_e^2 - t}{\sqrt{-t}\sqrt{4m_e^2 - t}} \log\frac{\sqrt{4m_e^2 - t} + \sqrt{-t}}{\sqrt{4m_e^2 - t} + \sqrt{-t}} - 1\Big). \tag{31}$$

As can be seen by Fig. 4, the approximate result derived in [23] provides a good estimate of the SAST cross section with an accuracy of order 5–10 % when the kinematical configuration proposed in ref. [13] ($0 \leq \vartheta_- \leq 20$ mrad, 250 MeV $\leq E_- \leq 440$ MeV) is assumed. In the limit of small electron scattering angles ($\vartheta \leq 2$ mrad) the relative deviation decreases as E_-^{max} increases, consistently with the soft, collinear and no–recoil approximation adopted in ref. [23].

The total cross section for photons emitted in the forward region is shown in Fig. 5. The results are obtained by integrating the photon energy E_γ over the range $\Delta E_\gamma = E_b - E_\gamma^{min}$ as a function of the minimum photon energy E_γ^{min}. The different curves correspond to ϑ_γ in the regions $0 \leq \vartheta_\gamma \leq 1$ mrad (dashed line), $0 \leq \vartheta_\gamma \leq 2$ mrad (dotted line), $0 \leq \vartheta_\gamma \leq 3$ mrad (dash–dotted line), $0 \leq \vartheta_\gamma \leq 8.5^o$ (solid line). The physical content of Fig. 5 is that the radiation is essentially emitted within a cone of half–opening angle of 2 mrad, as expected from the collinear nature of the bremsstrahlung mechanism.

Further numerical results for the total cross section of small angle electron–photon double tagging, of small–large and large–large electron–positron double tagging can be

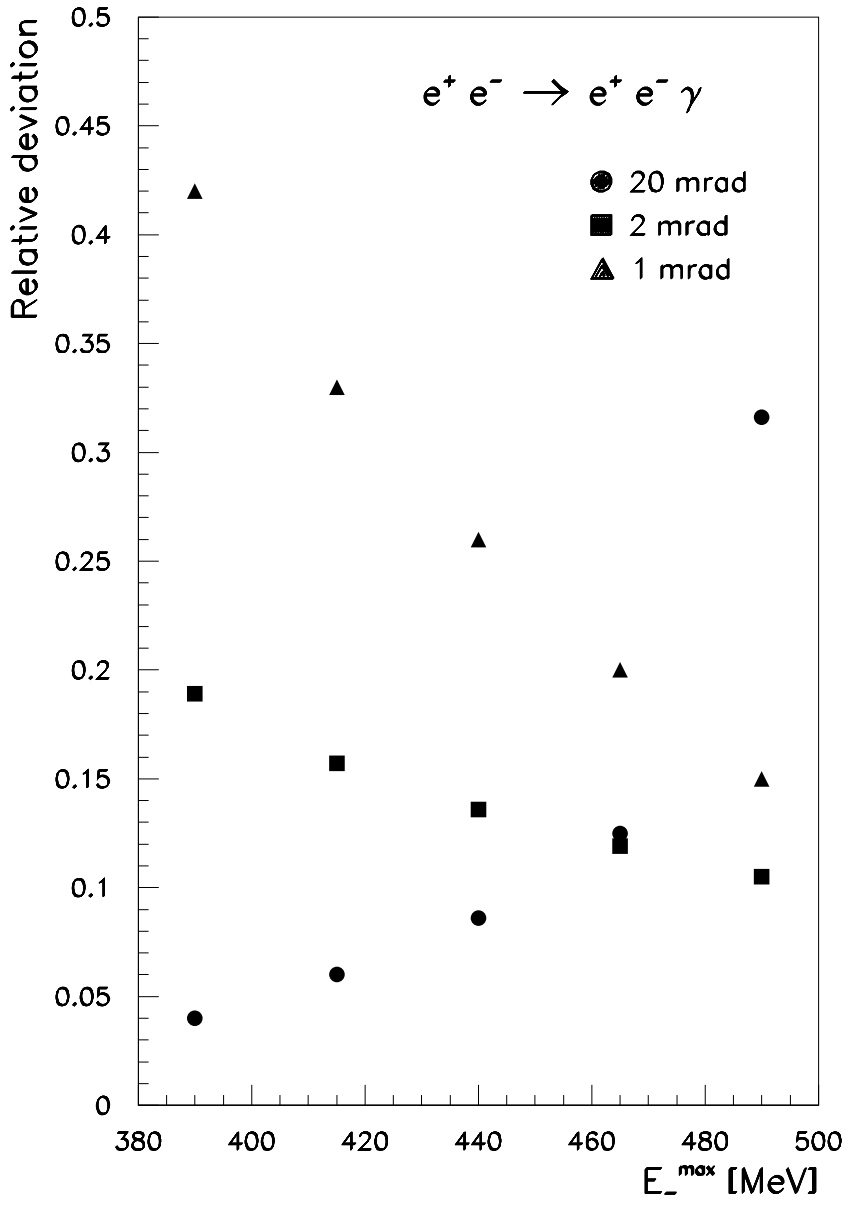

Figure 4: Comparison for the total cross section of small angle single tagging between the results of ref. [23] and ours obtained by integrating the electron scattering angle in the range $0 \leq \vartheta_- \leq 1$ mrad , $0 \leq \vartheta_- \leq 2$ mrad and $0 \leq \vartheta_- \leq 20$ mrad and the electron energy within $\Delta E_- = E_-^{max} - E_-^{min} = 190$ MeV, as a function of the maximum electron energy E_-^{max}. The relative deviation is defined as: $2\ (\sigma^{[23]} - \sigma)/(\sigma^{[23]} + \sigma)$.

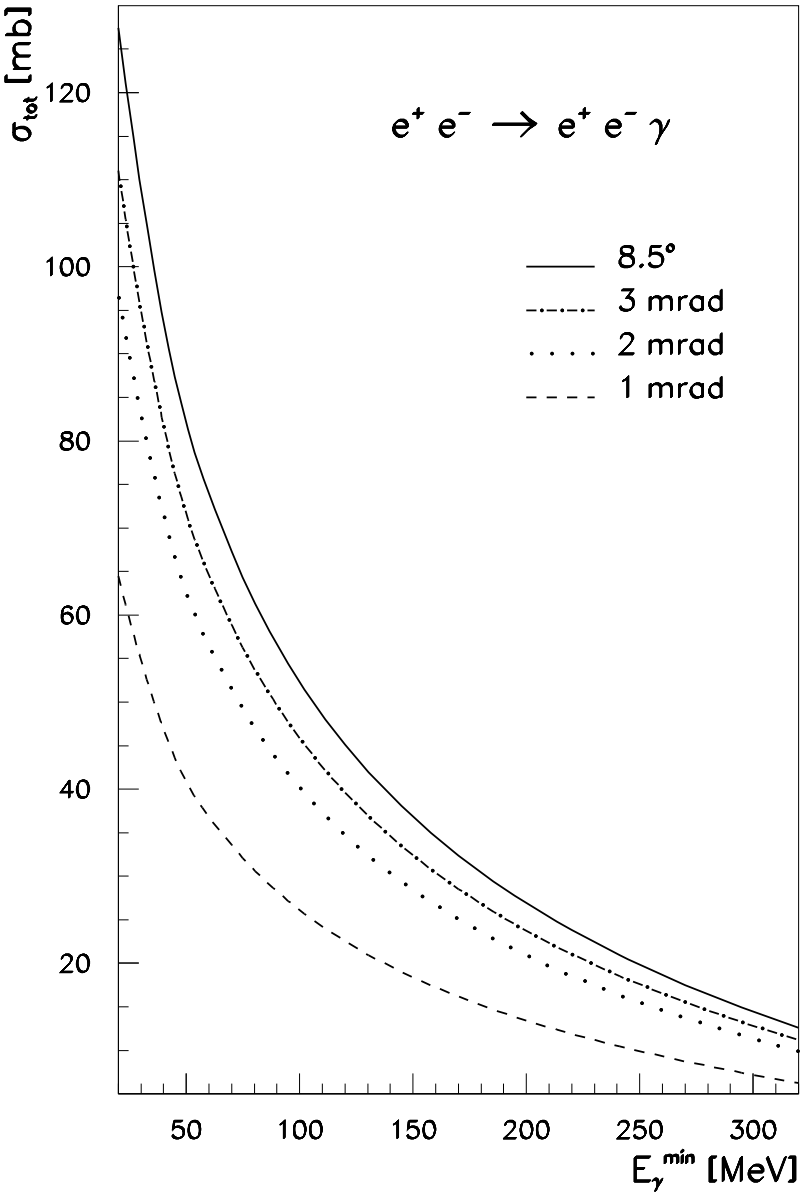

Figure 5: Total cross section for the photon in the forward region obtained by integrating ϑ_γ in the regions $0 \leq \vartheta_\gamma \leq 1$ mrad (dashed line), $0 \leq \vartheta_\gamma \leq 2$ mrad (dotted line), $0 \leq \vartheta_\gamma \leq 10$ mrad (dot–dashed line), $0 \leq \vartheta_\gamma \leq 8.5^o$ (solid line) and E_γ over the range $\Delta E_\gamma = E_b - E_\gamma^{min}$ as a function of the minimum photon energy E_γ^{min}.

found in [19]. Our results, obtained by the code `PHIPHI`, has been checked very recently by the Monte Carlo generator `BBBREM` [24] and found in very good agreement [25]. In particular, for the unconstrained kinematics, we also agree with the single photon spectrum and the total cross section derived in refs. [15, 16].

We would like to point out, in conclusion, that for the SLDT case, where for kinematical reasons no mass divergences appear, the ultrarelativistic matrix element of ref. [18] can be safely used. In the LLDT case mass divergences do appear but the condition $|t| \gg m^2$ is fulfilled so that complete CALKUL result do apply. In all the other cases (SAST, SADT, SAEPC and LS) one has both mass divergences and very small angles, so that the full matrix element of eq. (24), including quartic and sextic mass correction terms, must be used.

Acknowledgments

Part of the theoretical results on QED radiative corrections to e^+e^- collisions here summarized have been obtained in collaboration with G. Passarino whom we would like to thank. Many stimulating discussions with D. Babusci and A. Zallo about radiative Bhabha scattering at DAΦNE are acknowledged. We are also grateful to INFN, Sezione di Pavia, for having provided computer resources and, in particular, to V. Filippini and A. Fontana for having allowed the use of IBM RISC/350.

References

[1] M. Greco, G. Pancheri and Y. Srivastava, Nucl. Phys. B101 (1975) 234; Nucl. Phys. B171 (1980) 118.

[2] G. Montagna, O. Nicrosini, G. Passarino, F. Piccinini and R. Pittau, Nucl. Phys. B401 (1993) 3 and references therein.

[3] G. Montagna, O. Nicrosini and F. Piccinini, Phys. Rev. D48 (1993) 1021.

[4] G. Colangelo, S. Dubnička and M. Greco, *Radiative Corrections at DAΦNE*, The DAΦNE Physics Handbook, L. Maiani, G. Pancheri and N. Paver Eds., Vol. II, pg. 327.

[5] E. A. Kuraev and V. S. Fadin, Sov. J. Nucl. Phys. 41 (1985) 466;
G. Altarelli and G. Martinelli, *Physics at LEP*, CERN Report 86–02, J. Ellis and R. Peccei Eds. (Geneva 1986); see also:
F. A. Berends et al., *Z Physics at LEP1*, G. Altarelli, R. Kleiss and C. Verzegnassi eds., CERN 89–08, Vol. 1, (1989) 89 and references therein.

[6] O. Nicrosini and L. Trentadue, Phys. Lett. B196 (1987) 551; Z. Phys. C39 (1988) 479.
For a review see also:
O. Nicrosini and L. Trentadue, in *Radiative Corrections for e^+e^- Collisions*,

J. H. Kühn ed. (Springer, Berlin, 1989)25; in *QED Structure Functions*, G. Bonvicini ed., AIP Conf. Proc. No. 201 (AIP, New York,1990) 12; O. Nicrosini, ibidem 73.

[7] J. Collins, D. Soper and G. Sterman, in *Perturbative QCD*, A. H. Mueller ed. (World Scientific, Singapore, 1989) and references therein.

[8] F. Aversa and M. Greco, Phys. Lett. B228 (1989) 134; Phys. Lett. B271 (1991) 435 and references therein.

[9] G. Montagna, O. Nicrosini and G. Passarino, Phys. Lett. B309 (1993) 436.

[10] M. Cacciari, G. Montagna and O. Nicrosini, Phys. Lett. B274 (1992) 473. See also:
M. Caffo, R. Gatto and E. Remiddi, Phys. Lett. B139 (1984) 439; Nucl. Phys. B252 (1985) 378;
G. Sterman and S. Weinberg, Phys. Rev. Lett. 39 (1977) 1436;
J. Fleisher and F. Jegerlehner, Z. Phys. C26 (1985) 629;
M. Greco, Riv. Nuovo Cimento 11 (1988) no. 5.

[11] G. Montagna, O. Nicrosini, G. Passarino, F. Piccinini and R. Pittau, Comput. Phys. Commun. 76 (1993) 328.

[12] F. Anulli et al., The DAΦNE Physics Handbook, L. Maiani, G. Pancheri and N. Paver Eds., Vol. II, pg. 435.

[13] G. Alexander et al., *Two Photon Physics Capabilities of KLOE at DAΦNE*, LNF–93/030(P).

[14] KLOE, A General Purpose Detector for DAΦNE, LNF–92/019(R).

[15] G. Altarelli and F. Buccella, Nuovo Cimento 34 (1964) 1337;
G. Altarelli and B. Stella, Lett. Nuovo Cimento 9 (1974) 416.

[16] V. N. Baier, V. S. Fadin, V. A. Khoze and E. A. Kuraev, Physics Report 78 (1981) 293.

[17] A. D. Bukin and E. A. Kuraev, Sov. J. Nucl. Phys. 42 (1985) 431.

[18] F. A. Berends, R. Kleiss, P. De Causmaecker, R. Gastmans, W. Trooost and T. T. Wu, Nucl. Phys. B206 (1982) 61 and references therein. See also R. Gastmans and T. T. Wu, *"The Ubiquitous Photon: Helicity Method for QED and QCD"*, Oxford Science Pub., 1990.

[19] M. Greco, G. Montagna, O. Nicrosini and F. Piccinini, Phys. Lett. B318 (1993) 635.

[20] `SCHOONSCHIP`, *A Program for Symbol Handling* by M. Veltman, see H. Strubbe, Comp. Phys. Comm. 8 (1974) 1.

[21] R. Kleiss, Phys. Lett. B318 (1993) 217.

[22] G. Montagna, O. Nicrosini and F. Piccinini, Comp. Phys. Comm. 78 (1993) 155; erratum notice in Comp. Phys. Comm. 79 (1994) 351.

[23] G. Pancheri, Phys. Lett. B315 (1993) 477.

[24] R. Kleiss and H. Burkhardt, `BBBREM` – *Monte Carlo Simulation of Radiative Bhabha Scattering in the Very Forward Direction*, NIKHEF–H/94–01 and CERN SL/94–03, submitted to Comp. Phys. Comm.

[25] R. Kleiss, private communication.